

**This item is the archived peer-reviewed author-version of:**

Occurrence and contamination profile of legacy and emerging per- and polyfluoroalkyl substances (PFAS) in Belgian wastewater using target, suspect and non-target screening approaches

**Reference:**

Jeong Yunsun, da Silva Katyeny Manuela, Iturrospe Elias, Fujii Yukiko, Boogaerts Tim, van Nuijs Alexander, Koelmel Jeremy, Covaci Adrian.- Occurrence and contamination profile of legacy and emerging per- and polyfluoroalkyl substances (PFAS) in Belgian wastewater using target, suspect and non-target screening approaches

Journal of hazardous materials - ISSN 1873-3336 - 437(2022), 129378

Full text (Publisher's DOI): <https://doi.org/10.1016/J.JHAZMAT.2022.129378>

To cite this reference: <https://hdl.handle.net/10067/1892330151162165141>

1 **Occurrence and contamination profile of legacy and emerging per- and**  
2 **polyfluoroalkyl substances (PFAS) in Belgian wastewater using target, suspect**  
3 **and non-target screening approaches**

4

5 Yunsun Jeong<sup>a,\*</sup>, Katyeny Manuela Da Silva<sup>a</sup>, Elias Iturrospe<sup>a,b</sup>, Yukiko Fujii<sup>a,c</sup>, Tim Boogaerts<sup>a</sup>,  
6 Alexander L.N. van Nuijs<sup>a</sup>, Jeremy Koelmel<sup>d</sup>, Adrian Covaci<sup>a</sup>

7

8 \*Corresponding author

9

10 <sup>a</sup>Toxicological Centre, Department of Pharmaceutical Sciences, University of Antwerp,  
11 Universiteitsplein 1, 2610 Wilrijk, Belgium

12 <sup>b</sup>Department of *In Vitro* Toxicology and Dermato-Cosmetology, Free University of Brussels,  
13 Laarbeeklaan 103, 1090 Brussels, Belgium

14 <sup>c</sup>Department of Pharmaceutical Sciences, Daiichi University of Pharmacy, 22-1 Tamagawa-  
15 cho, Minami-ku, Fukuoka 815-8511, Japan

16 <sup>d</sup>School of Public Health, Yale University, New Haven, Connecticut 06520, United States

17 **Abstract**

18 With the growing concern regarding the health risks of per- and polyfluoroalkyl substances  
19 (PFAS), there is an increasing demand for the identification of emerging PFAS. This study  
20 provides a comprehensive investigation of legacy and emerging PFAS in 16 wastewater  
21 treatment plants (WWTPs) in Belgium using target, suspect, and non-target screening  
22 methods. Perfluorobutanoic acid (PFBA) and perfluoropentanoic acid (PFPeA) were the  
23 dominant compounds in most locations, whereas perfluorooctanoic acid (PFOA) was the most  
24 predominant PFAS in WWTP Deurne (Antwerp region). Using a suspect screening approach,  
25 14 PFAS were annotated as confidence level (CL) of 4 or higher and 4 PFAS were annotated  
26 as CL 2a and 2b, including aqueous film forming foam (AFFF)-derived PFAS. The compound  
27 group of n:3 unsaturated fluorotelomer carboxylic acid was found using non-target screening  
28 in the wastewater from WWTP Deurne. Population exposure in a catchment area estimated  
29 using population-normalized mass loads (PNML) showed the highest value in the catchment  
30 area of WWTP Deurne, implying a potentially higher exposure to PFAS in this community.

31

32 **Keywords** Belgium, High-resolution mass spectrometry (HRMS), Influent wastewater, Non-  
33 target screening, PFAS

34 **Environmental Implication**

35 Per- and polyfluoroalkyl substances (PFAS) are a group of chemicals that have been receiving  
36 global attention due to their strong persistence, bioaccumulation potential, and toxicity. This  
37 study conducted comprehensive monitoring of a broad range PFAS in Belgian wastewater.  
38 Target, suspect, and non-target analytical approaches were used to identify emerging PFAS,  
39 examine contamination profiles, and to assess population exposure. The outcome of this study  
40 can be utilized to build new monitoring strategies for emerging PFAS and to characterize  
41 regions at elevated exposure to protect local health.

## 42 **1. Introduction**

43 Poly- and perfluoroalkyl substances (PFAS) are a class of synthetic chemicals that  
44 have been used in a wide range of industrial and commercial products since the 1950s (Evich  
45 et al., 2022; Giesy and Kannan, 2002; Lindstrom et al., 2002; Wang et al., 2017). Due to their  
46 unique physicochemical properties (i.e., strong C-F bonds and repellency to water and oil),  
47 PFAS have been applied as surfactants, lubricants, mist suppressants, fast-food contact  
48 materials, cosmetics, and aqueous film-foaming foams (AFFFs) (Buck et al., 2011). The most  
49 well-known PFAS classes are perfluoroalkyl sulfonic acids (PFSA) and perfluoroalkyl  
50 carboxylic acids (PFCA), which are represented by perfluorooctane sulfonic acid (PFOS) and  
51 perfluorooctanoic acid (PFOA), respectively. Due to the strong persistence, bioaccumulation  
52 potential, and toxicity (i.e., thyroid dysfunction (Aimuzi et al., 2019), low birth weight (Wikström  
53 et al., 2020), and immune function disorders (Chang et al., 2016; Wen et al., 2019)), PFOS,  
54 PFOA and their salts were designated as persistent organic pollutants (POPs) under the United  
55 Nations Environment Programme (UNEP) Stockholm Convention (UNEP, 2019a, 2009). In line  
56 with this regulation, in 2019, the POPs review committee of the Stockholm Convention adopted  
57 a new decision to add perfluorohexane sulfonic acid (PFHxS) and its salts to the POPs list  
58 Annex A (UNEP, 2019b).

59 With respect to the global regulation of PFOS and PFOA, industries have claimed to  
60 shift their production of fluorinated compounds to less persistent and bioaccumulative PFAS,  
61 such as shorter chain PFAS (i.e., perfluorobutane sulfonic acid (PFBS) and perfluorobutanoic  
62 acid (PFBA)) and/or fluoroether replacements, such as GenX (hexafluoropropylene oxide  
63 dimer acid; HFPO-DA), ADONA (dodecafluoro-3H-4,8-dioxanonanoate), and F-53B (6:2  
64 chlorinated polyfluoroalkyl ether sulfonate). However, shorter chain PFAS and alternatives are  
65 still of concern, because they are still recalcitrant, highly mobile or comparably persistent and  
66 toxic to PFOS and PFOA (Gaballah et al., 2020; Gordon, 2011; Munoz et al., 2019; Wang et  
67 al., 2013). In addition to the known alternatives, fluorine mass balance studies have recently  
68 reported that known PFAS (routinely monitored PFAS) only account for 2–44% of extractable  
69 organic fluorine (EOF), encouraging paradigm changes in scientific research to broad

70 screening of PFAS using suspect and/or non-target screening (Cousins et al., 2020;  
71 Kwiatkowski et al., 2020; Ruan and Jiang, 2017; Yeung et al., 2013).

72 High resolution mass spectrometry (HRMS) instruments, such as time-of-flight MS  
73 (TOF-MS) and Orbitrap MS, offer the opportunity to discover and identify unknown chemicals  
74 by providing resolving power and mass accuracy (Barzen-Hanson et al., 2017a; Liu et al.,  
75 2019). Recent studies have found previously unreported PFAS in various matrices, such as  
76 wastewater released from a fluorochemical manufacturing park (Liu et al., 2015), AFFFs-  
77 impacted groundwater (Barzen-Hanson et al., 2017a), wastewater treatment plant (WWTP)  
78 receiving large AFFF-inputs (Houtz et al., 2018), wastewater from a fluorochemical  
79 manufacturing park (Wang et al., 2018), fire-fighting foam impacted water (Yukioka et al., 2020),  
80 airborne particulate matter (Yu et al., 2018), and wastewater from electronics fabrication  
81 facilities (Jacob et al., 2021a) using suspect and non-target approaches. However, to the best  
82 of our knowledge, we are only aware of one study has performed a non-target analysis of  
83 PFAS in municipal wastewaters (Wang et al., 2020) despite of the important role of WWTPs  
84 as an indicator of regional contamination patterns and domestic exposure routes. Municipal  
85 wastewater has been successfully utilized to assess human exposure to chemicals by using a  
86 population-normalized mass load (PNML) (Choi et al., 2018).

87 Non-target analysis of PFASs has been performed using mass defect (i.e.,  $< 0.15$  or  
88  $> 0.85$ ) filtering accompanied with homologue analysis by repeating moiety patterns (i.e.,  $\text{CF}_2$ ,  
89  $\text{CF}_2\text{CF}_2$ , and  $\text{CF}_2\text{O}$ ) or fragment ion flagging (Liu et al., 2015). Non-target screening of PFAS  
90 is challenging because of the sophisticated data analysis procedure and absence of  
91 generalized workflow. In previous studies, acquired data from HRMS was processed using R  
92 packages (e.g., Package 'nontarget' (Loos and Singer, 2017) or in-house script (Wang et al.,  
93 2021)), MATLAB, or Excel, which requires specific training and expertise and/or involve time-  
94 consuming manual identification.

95 In the present study, we used a newly developed software 'FluoroMatch 2.0' for  
96 suspect and non-target screening of PFAS (Koelmel et al., 2020). The FluoroMatch software  
97 accurately annotates PFAS in a suspect screening fashion and contains fragmentation rules

98 for about 7,000 PFAS species across 70 classes. Furthermore, FluoroMatch performs peak  
99 picking, blank feature filtering, mass defect filtering, homologue analysis using CF<sub>2</sub>-normalized  
100 Kendrick mass defect (or any other repeating unit), retention time (RT) order within homologue  
101 groups, fragment screening (777 F-containing fragments), and *in silico* MS/MS library matching  
102 applied to the suspect list from US CompTox 'PFAS master list' for annotation. The software  
103 also assigns a confidence level for each feature by its scoring system based on the levels  
104 proposed by Schymanski et al. (2014). With emerging PFAS being a growing concern,  
105 FluoroMatch is a user-friendly and effective approach for the identification and the build-up of  
106 an extensive database on PFAS. In recent studies, FluoroMatch showed good performance  
107 for suspect and non-target analysis of PFAS in comparison with other software (i.e., Compound  
108 Discoverer) (Jacob et al., 2021b; Nason et al., 2021).

109 This study aims to investigate the occurrence and contamination profile of a broad  
110 range of PFAS in influent wastewater from 16 WWTPs in Belgium using target, suspect, and  
111 non-target screening approaches. Also, the estimation of population exposure in the catchment  
112 area has been used to identify regions at elevated risk. Additionally, the successful application  
113 of FluoroMatch 2.0 for suspect and non-target screening of PFAS in this study will provide  
114 guidance for further use of the software for extensive PFAS research. To the best of our  
115 knowledge, this is the first report on the suspect and non-target analysis of PFAS in Belgian  
116 influent wastewater.

117

## 118 **2. Materials and Methods**

### 119 *2.1. Sample Collection*

120 Daily 24-h composite influent wastewater samples were collected from 16 Belgian  
121 WWTPs (names given in English) including Aartselaar, Antwerp (North and South), Boom,  
122 Bruges, Deurne, Dendermonde, Genk, Ghent, Hasselt, Houthalen-Helchteren, Leuven,  
123 Mechelen, Sint-Niklaas, Turnhout, and Brussels-North regions during autumn (September and  
124 October), 2020 (**Figure S1**). For WWTP Brussels-North, influent wastewater samples collected  
125 in 2013, 2015, 2016, and 2017 were available for an overview of contamination pattern

126 changes during the past years. Detailed information on wastewater samples such as sampling  
127 months and dates, flow rate, and population equivalents are presented in **Table S1**.  
128 Wastewater samples were collected in high-density polyethylene (HDPE) bottles and stored at  
129 -20 °C until analysis.

130

## 131 *2.2. Sample Preparation*

132 A volume of 250 mL of each influent wastewater sample was transferred to pre-  
133 cleaned 50 mL polypropylene tubes. Samples were centrifuged for 10 min at 2465 g and an  
134 PFAS internal standard mixture (12.5 ng) was added. Detailed information on reference  
135 standards of PFAS used in this study are presented in **Table S2–S3**.

136 Optimization of the sample extraction method (cartridge selection) and suppliers of  
137 chemicals are described in Supporting Information and **Table S4**. Solid phase extraction (SPE)  
138 of wastewater samples was performed using Oasis HLB (6 mL, 500 mg) and Oasis WAX (6  
139 mL, 150 mg) cartridges. Prior to extraction, HLB cartridges were conditioned sequentially with  
140 10 mL of methanol (MeOH) and 10 mL of ultrapure water, while WAX cartridges were  
141 conditioned with 4 mL 0.5% (v/v) NH<sub>4</sub>OH in MeOH, 4 mL MeOH, and 4 mL of ultrapure water.  
142 After connecting the cartridges (HLB top and WAX bottom), wastewater samples (250 mL)  
143 were loaded into HLB to WAX cartridges sequentially under vacuum (1 drop/sec), then the  
144 cartridges were disconnected and washed with 10 mL of ultrapure water for the HLB cartridge  
145 and 4 mL of 25 mM sodium acetate buffer (pH 4) for the WAX cartridge considering the different  
146 sorbent types. After reaching dryness under vacuum, cartridges were eluted with 10 mL of  
147 MeOH (HLB) or 8 mL 0.5% (v/v) NH<sub>4</sub>OH in MeOH (WAX). Extracts were combined and  
148 evaporated under a gentle nitrogen stream until dryness (at 30 °C) and then reconstituted in  
149 500 µL of H<sub>2</sub>O/MeOH (10/90, v/v). Samples were centrifuged for 10 min at 3220 g and  
150 transferred to polypropylene vials for instrumental analysis.

151

## 152 *2.3. Instrumental analysis*



153 For target analysis, an Agilent 1290 Infinity ultra-high performance liquid  
154 chromatograph (UHPLC; Agilent Technologies, Santa Clara, CA, USA) interfaced with an  
155 Agilent 6495 triple quadrupole mass spectrometer (MS/MS; Agilent Technologies) was  
156 operated in electrospray ionization (ESI) negative polarity and target PFAS were monitored  
157 with multiple reaction monitoring (MRM) mode. Chromatographic separation was performed  
158 by a Zorbax Eclipse Plus RRHD C18 column (2.1 × 100 mm, particle size: 1.8 μm) connected  
159 with a guard column (Eclipse Plus C18, 2.1 × 5 mm, 1.8 μm). The mobile phases consisted of  
160 (a) 2 mM ammonium acetate in water and (b) MeOH with a flow rate of 0.25 mL/min. The  
161 detailed LC conditions, source parameters and MRM transitions are presented in **Table S5–**  
162 **S6**.

163 Suspect and non-target analysis was performed with an Agilent 1290 Infinity UHPLC  
164 coupled with an Agilent 6560 quadrupole time-of-flight mass spectrometry (QTOF-MS; Agilent  
165 Technologies). The UHPLC analytical condition and mobile phases were consistent to target  
166 analysis. Data acquisition was accomplished using ESI negative mode in full scan and iterative  
167 data-dependent acquisition modes (selection of 10 precursors) operated at a 2 GHz extended  
168 dynamic range mode with mass range  $m/z$  1700. Detailed information on QTOF-MS acquisition  
169 parameters is presented in **Table S7**. During the runs, real-time calibration was performed by  
170 infusing internal reference masses (lock mass) using purine ( $m/z$  119.0363) and hexakis (1H,  
171 1H, 3H-tetrafluoropropoxy) phosphazine ( $m/z$  980.0163).

172

#### 173 *2.4. Quality control and quality assurance (QA/QC)*

174 To avoid contamination during sample preparation, all experimental apparatus were  
175 cleaned 2–3 times with MeOH in prior to usage. Limit of quantification (LOQ) values and  
176 linearity of calibration curves ( $R^2$ ) applied in target analysis are presented in **Table S6**.  
177 Concentrations below LOQ values were treated as zero to avoid overestimation due to a lower  
178 concentration range of PFAS (Baccarelli et al., 2005). In the QTOF-MS analysis, known  
179 amounts of a native PFAS standard mixture (0.1, 0.5, 1, 5, and 10 ng/mL) were injected to  
180 check the instrumental sensitivity and mass accuracy (**Table S8**). All compounds in the native

181 standard mixture, including 4 sulfonates (C4, C6, C8, and C10) and 11 carboxylates (C4–C14)  
182 were detected with concentrations above 0.1 ng/mL, except for PFBA, which was found above  
183 5 ng/mL. To avoid cross-contamination between samples, the injection needle was washed for  
184 1 min with 50% isopropanol (IPA) in water (v/v) after every injection and a MeOH solvent blank  
185 was injected between wastewater sample injections of each site. Instrumental sensitivity was  
186 examined by injection of internal standard mixture (25 ng/mL) after every 15 samples and they  
187 showed consistent peak abundances and mass accuracies. The MeOH solvent blank and  
188 procedural blank did not show any quantifiable levels of targeted and newly identified PFAS,  
189 except for 6:2 fluorotelomer sulfonate (6:2 FTS). The area of 6:2 FTS in blank has been  
190 subtracted from the wastewater samples. Detailed QA/QC procedures and results including  
191 matrix effect test (**Table S9, Figure S2**) are presented in Supporting Information.

192

### 193 *2.5. Data analysis*

194 *Target analysis.* A total of 34 PFAS were quantified using Agilent MassHunter Quantitative  
195 Analysis 10.0 software. Compounds without corresponding labeled internal standard were  
196 quantified with the most similar labeled compound considering the molecular weight, RT, and  
197 functional group (**Table S6**).

198 *Suspect and non-target screening.* The data analysis workflows for suspect and non-targeted  
199 screening of PFASs in wastewater are summarized in **Figure 1** and described in **Supporting**  
200 **information** (Data analysis). Prior to data analysis, the workflow was validated by applying  
201 native PFAS standard injections to the entire software process and the homologue groups  
202 (PFASs and PFCAs) were successfully annotated and categorized (**Table S10**).

203 Data preprocessing was performed using the open-source software MS-DIAL (version  
204 4.60) (Tsugawa et al., 2015) and the detailed parameters are presented in **Table S11**. The  
205 feature table obtained from MS-DIAL, which includes peak alignment ID, average *m/z*, average  
206 RT, and peak area, and the data-dependent acquisition files for each site were processed with  
207 FluoroMatch 2.0 Modular with the following criteria; (1) RT tolerance:  $\pm 0.3$  min; (2) ppm window:  
208 10 ppm; (3) mass accuracy: 0.01 Da; (4) MS/MS isolation window: 0.05 Da; (5) MS/MS

209 intensity cutoff (minimum signal intensity cutoff): 10; (6) mass defect filtering: -0.11 to 0.12.  
210 After processing the dataset, features classified as level 'E' (not likely PFAS) according to the  
211 internal scoring system of FluoroMatch 2.0 (**Table S12**) and features with Kendrick mass defect  
212 value between 0.15 to 0.85 were excluded. As a result, a total of 8,706 aligned features were  
213 classified as potential PFAS.

214 For suspect screening, the *m/z* values of features were matched with the PFAS Master  
215 List (included in FluoroMatch) and were sorted by detected frequency (> 60% of the sampling  
216 sites). The peak shapes of matched features were examined with MS-DIAL. With the selected  
217 features, the isotopic pattern and MS/MS fragmentation pattern were manually inspected with  
218 Agilent MassHunter Qualitative Analysis 7.0. Additionally, to include a recent literature finding,  
219 the suspect list provided by Liu et al. (2019) which merged previously reported PFAS  
220 homologue groups and lists of novel PFAS in recent wastewater studies (Jacob et al., 2021a;  
221 Wang et al., 2020, 2018) were also applied to Belgian wastewater.

222 Non-target screening was conducted by investigating assigned homologue groups  
223 provided by FluoroMatch 2.0. Homologue groups which had features characterized with  
224 diagnostic fragment ions (i.e.,  $\text{SO}_3^-$ ,  $\text{CF}_2^-$ ,  $\text{C}_2\text{F}_5^-$ , etc.) or consecutive RT for over three  
225 compounds were sorted for further investigation. Each feature's peak shape, RT and isotopic  
226 patterns were manually checked with MassHunter Qualitative Analysis 7.0.

227 With the compounds identified by suspect and non-target screening, the confidence  
228 level (CL) of compound identification was determined based on the recommendation of  
229 Schymanski et al. (2014), which consists of CL 1 (confirmed structure by reference standard),  
230 CL 2 (probable structure by library matching; 2a or diagnostic evidence; 2b), CL 3 (tentative  
231 candidates identified with substructure, class, etc.), CL 4 (unequivocal molecular formula  
232 without sufficient structure evidence), and CL 5 (mass of interest) (Schymanski et al., 2014).

233 The semi-quantification has been performed for newly found PFAS based on the  
234 method described in Jacob et al. (2021a). Initially, individual newly identified PFAS were  
235 matched with target PFAS quantified by LC-MS/MS according to molecular weight, RT, and  
236 functional group similarity. As a further step, the ratio of newly identified PFAS peak area

237 divided by that of matched target PFAS was then multiplied by the concentration of the target  
238 PFAS quantified by LC-MS/MS to generate semi-quantitative concentration values.

239 The population exposure to PFAS in catchment area was estimated using population  
240 normalized mass load (PNML). Total mass load (g/day) was defined as the PFAS measured  
241 concentration multiplied by the daily service volume on the sampling day for each WWTP and  
242 PNML of PFAS in influent wastewater were calculated as total mass load divided by the served  
243 population. The inputs used for estimating total mass load and PNML are presented in **Table**  
244 **S1**.

245

### 246 **3. Results and discussion**

#### 247 *3.1. Target analysis*

248 In total, 34 PFAS including groups of sulfonates, carboxylates, sulfonamides,  
249 sulfonamido acetic acids, sulfonamido ethyl alcohols, unsaturated carboxylates, phosphonic  
250 acids, fluorotelomer sulfonates, and ether-substituted PFAS alternatives, such as HFPOs,  
251 ADONA, and F-53B, were analyzed in Belgian wastewaters. Concentration, mass loads, and  
252 contamination patterns of measured PFAS in 16 municipal WWTPs and historical Brussels  
253 WWTP influent (2013–2020) are presented in **Table S13**, **Figure 2a**, and **2b**. In our study,  
254 comparisons of PFAS levels and composition between WWTPs were conducted on a total  
255 mass load balance to account for variation in flow rates associated with specific sampling dates.

256 In all 16 WWTPs, PFBS, PFOS, PFBA, PFPeA, PFOA, PFDA and 8:2 FTS were  
257 observed and PFHxS, PFHxA, PFHpA, and PFNA were detected in over 80% of the sampling  
258 sites, whereas other compounds showed lower detection frequency (< 5%). These results  
259 indicate continuous introduction of legacy PFAS including PFOS and PFOA to Belgian WWTPs  
260 in spite of global regulation. The highest mass load of total legacy PFAS was found in the  
261 WWTP Deurne (133 g/day), which covers wastewater from the outer districts of Antwerp,  
262 followed by WWTPs of Bruges (8.89 g/day), Ghent (5.06 g/day), Antwerp South (3.41 g/day),  
263 Dendermonde (2.93 g/day), and Turnhout (2.46 g/day). At the majority of the sites, the  
264 dominant PFAS were shorter chain PFAS including PFBA (3.2–54%), PFPeA (5.8–78%), and

265 PFBS (0.2–29%), whereas PFOA represented approximately 80% of total PFAS in WWTP  
266 Deurne. This result indicates that there might be specific sources of PFOA or its precursor (i.e.,  
267 fluoropolymer, fluorotelomer-based substances such as fluorotelomer alcohols; FTOHs, etc.)  
268 nearby WWTP Deurne. However, due to the limited information on the type of wastewater (i.e.,  
269 industrial) input to WWTPs, we could not conduct in-depth investigation on the possible  
270 sources of PFOA. Consistent with our results, Phong Vo et al. (2020) reported the dominance  
271 of shorter chain PFAS in European countries, United States, and Australia associated with the  
272 regulation effect, while PFOS and PFOA are still a major PFAS in developing countries (Lenka  
273 et al., 2021; Phong Vo et al., 2020).

274 In the WWTP Brussels-North, the largest WWTP in Belgium, retrospective time point  
275 samples collected in 2013, 2015, 2016, 2017, and 2020 were analyzed to estimate the  
276 temporal changes of PFAS contamination pattern. The total PFAS mass loads varied  
277 throughout the sampling years and ranged from 13.2 g/day to 69.7 g/day. The relative  
278 contribution of individual PFAS showed a slight decreasing trend of PFOS, PFHpA, and PFOA  
279 from 2013 to 2020, yet those trends were not statistically significant (**Figure S3**). The PFAS  
280 contamination pattern changed between the year of 2015 and 2016, from the dominance of  
281 PFOS (32–46%) in 2013 and 2015 wastewaters to PFPeA and PFBA (11–74%) in 2016, 2017,  
282 and 2020 (**Figure 2b**) implying that the sources of PFAS in Brussels region may have changed  
283 during those years. However, due to the limited sample size, the result might not reflect the  
284 actual PFAS contamination trend in WWTP Brussels. To validate the time trend of PFAS  
285 contamination, additional retrospective wastewater samples should be analyzed.

286

### 287 *3.2. Suspect Screening of PFAS*

288 Molecular formulas, matching scores (obtained by software), compound names  
289 (matched name with suspect list), and identification confidence levels of PFAS that identified  
290 by suspect screening are presented in **Table 1 and Table S14**. In total, 14 compounds were  
291 annotated as CL 4 or higher based on exact mass matching, detection frequency (> 60%),  
292 isotopic pattern, and available MS/MS fragmentation patterns. Among them, 4 compounds

293 were classified as CL 2a and 2b and 4 compounds were identified as CL 3 while others  
294 remained as CL 4.

295 *CL 2a and 2b.* In Belgian influent wastewaters, two compounds with chemical formulas  
296 of  $C_{15}H_{18}F_{13}NO_5S_2$  ( $m/z$  602.0339; 6:2 fluorotelomer sulfinyl amido sulfonic acid; 6:2 FtSOAoS)  
297 and  $C_{15}H_{18}F_{13}NO_6S_2$  ( $m/z$  618.0288; 6:2 fluorotelomer sulfonyl amido sulfonic acid; 6:2  
298 FtSO<sub>2</sub>AoS) were identified as CL 2a. The diagnostic MS/MS fragments for each compound  
299 were  $[M-H]^-$ ,  $[C_7H_{14}NO_5S_2]^-$ ,  $[C_7H_{12}NO_4S]^-$ , and  $[C_4H_{10}NO_3S]^-$  for  $C_{15}H_{18}F_{13}NO_5S_2$  (**Figure S4a**),  
300 and  $[M-H]^-$ ,  $[C_7H_{12}NO_4S]^-$ ,  $[C_4H_{10}NO_3S]^-$ , and  $[O_3S]^-$  for  $C_{15}H_{18}F_{13}NO_6S_2$  (**Figure S4b**). Previous  
301 studies reported the occurrence of  $C_{15}H_{18}F_{13}NO_5S_2$  and  $C_{15}H_{18}F_{13}NO_6S_2$  in U.S. WWTPs  
302 (focusing on AFFF-derived PFAS) (Houtz et al., 2018), AFFF, and Commercial Surfactant  
303 Concentrates (D'Agostino and Mabury, 2014). The MS/MS fragmentation patterns obtained  
304 from our study were consistent to previous findings, which enables compound annotation as  
305 CL2a.

306 A compound with formula  $C_3H_2F_6O_4S$  ( $m/z$  246.9498; 1:2 H-substituted perfluoroalkyl  
307 ether sulfonate) was identified based on the findings in Chinese municipal wastewater (Wang  
308 et al., 2020). The author provided the potential name of this compound as 1:2 H-substituted  
309 perfluoroalkyl ether sulfonate (1:2 H-PFESA) and the structure was confirmed by fragment ions  
310 of  $[C_3F_5O_4S]^-$ ,  $[C_3HF_6O]^-$ ,  $[C_3F_5O]^-$ ,  $[C_2F_5O]^-$ ,  $[HO_3S]^-$ , and  $[CF_3]^-$  which were consistent with our  
311 findings (**Figure S5a**). In the study of Wang et al. (2020), 1:2 H-PFESA was identified by  
312 homologue analysis and the major compound of that homologue group is 6:2 H-PFESA  
313 (dominant transformation product of 6:2 Cl-PFESA), however, those compounds were not  
314 observed in Belgian wastewater. Wang et al. (2020) also mentioned that  $C_3H_2F_6O_4S$  might not  
315 have consistently a H atom position with other homologues observed. Based on these  
316 concerns, despite of the similarity in major MS/MS fragmentation pattern, this compound  
317 remained as CL 2b. Compound  $C_8HF_{18}NO_4S_2$  ( $m/z$  579.8974; bis(1,1,2,2,3,3,4,4,4-nonafluoro-  
318 1-butanefluoronyl)-imide; **Figure S5b**) was also identified to CL2b by confirming the structure  
319 with fragmentation ions of  $[M-H]^-$ ,  $[C_4F_9NO_2S]^-$ ,  $[FO_2S]^-$ , and  $[NO_2S]^-$ . Until now, only one study  
320 have reported the detection of homologue group of bisperfluoroalkane sulfonylimides including

321 C<sub>8</sub>HF<sub>18</sub>NO<sub>4</sub>S<sub>2</sub> from the mice dosed with an AFFF primarily containing electrochemically  
322 fluorinated PFAS (McDonough et al., 2020). To the best of our knowledge, this is the first report  
323 on environmental occurrence of bis-(1,1,2,2,3,3,4,4,4-nonafluoro-1-butanefluoro-1-butanesulfonyl)-imide.

324 CL 3. Four compounds were assigned as CL 3 with the characterization of  
325 distinguishable MS isotopic patterns, such as Cl or Br ions. The MS/MS fragments were not  
326 obtained due to a lower peak abundance. C<sub>5</sub>H<sub>3</sub>Cl<sub>2</sub>F<sub>3</sub>O (*m/z* 204.9467; 2-chloro-2,3,3-  
327 trifluorocyclobutane-1-carbonyl chloride), C<sub>6</sub>H<sub>5</sub>Cl<sub>2</sub>F<sub>3</sub>O (*m/z* 218.9589; 2-chloro-2,3,3-trifluoro-  
328 1-methylcyclobutane-1-carbonyl chloride), C<sub>5</sub>H<sub>6</sub>BrF<sub>4</sub>NO<sub>2</sub> (*m/z* 265.9419; 2-bromo-2,3,3,3-  
329 tetrafluoro-N-methoxy-N-methylpropanamide) and C<sub>8</sub>H<sub>4</sub>BrF<sub>5</sub>O (*m/z* 288.9277; 1-bromo-4-  
330 (pentafluoroethoxy) benzene) were characterized by unique MS isotopic patterns derived by  
331 chlorine and bromine, with the highest isotopic pattern matching score over 90 (**Figure S6**).

332 CL 4. Six compounds were identified as CL 4 by molecular formula extraction with a  
333 higher compound matching score (average > 80 and highest > 90). Compounds with the  
334 formulas C<sub>4</sub>H<sub>2</sub>F<sub>8</sub>O<sub>3</sub>S (*m/z* 280.9517) and C<sub>7</sub>H<sub>6</sub>F<sub>9</sub>NO<sub>4</sub>S (*m/z* 369.9808) were found with a  
335 suspect screening list of newly found PFAS reported in recent non-target PFAS studies (Liu et  
336 al., 2019). The potential names of those compounds are 1,1,2,2,3,3,4,4-octafluorobutane-1-  
337 sulphonic acid (H-PFSA) and methylperfluorobutane sulfonamidoacetic acid (MeFBSAA;  
338 C<sub>7</sub>H<sub>6</sub>F<sub>9</sub>NO<sub>4</sub>S), respectively. In previous studies, the formulae C<sub>4</sub>H<sub>2</sub>F<sub>8</sub>O<sub>3</sub>S and C<sub>7</sub>H<sub>6</sub>F<sub>9</sub>NO<sub>4</sub>S  
339 were observed from downstream of manufacturing facilities near Decatur (Newton et al., 2017)  
340 and C<sub>4</sub>H<sub>2</sub>F<sub>8</sub>O<sub>3</sub>S was also detected in AFFF formulations (Barzen-Hanson et al., 2017) and river  
341 and drinking water near a fluorochemical production plant in the Netherlands (Gebbink et al.,  
342 2017). This finding indicates that the continuous update of PFAS suspect list is necessary  
343 based on recent scientific findings to investigate broader range of emerging PFAS.

344 With the FluoroMatch workflow, four other CL 4 compounds, C<sub>8</sub>HF<sub>15</sub>O<sub>3</sub>S (*m/z*  
345 460.9323; perfluoro-4-(perfluoroethyl)-cyclohexylsulfonic acid), C<sub>11</sub>H<sub>12</sub>F<sub>11</sub>NO<sub>4</sub>S (*m/z* 462.0265;  
346 ethyl N-ethyl-N-(1,1,2,2,3,3,4,4,5,5,5-undecafluoropentane-1-sulfonyl)glycinate,  
347 C<sub>15</sub>H<sub>19</sub>F<sub>13</sub>N<sub>2</sub>O<sub>4</sub>S (*m/z* 569.0777; 6:2 fluorotelomer sulfonamide betaine; 6:2 FTAB) and  
348 C<sub>15</sub>H<sub>18</sub>F<sub>13</sub>NO<sub>4</sub>S<sub>2</sub> (*m/z* 586.0378; 6:2 fluorotelomer thioether amido sulfonic acid; 6:2 FtTAoS)

349 were identified. The formula  $C_8HF_{15}O_3S$  was also annotated as unsaturated (double-bond)  
350 perfluoroalkyl sulfonic acid in the Barzen-Hanson et al. (2017), however, due to the unclear  
351 MS/MS spectra derived from low peak abundance, we could not confirm the final molecular  
352 structure.

353 In previous studies, 6:2 FTAB was observed in wastewater influent from a regional city  
354 catchment of Australia (Gallen et al., 2022), urban surface water in Canada (Agostino and  
355 Mabury, 2017), river and seawater samples in China (Chen et al., 2020), and sewage sludge,  
356 biowaste compost, and municipal solid wastes (Munoz et al., 2021) implied the widespread  
357 detection of AFFF-derived PFAS in the environment. Especially, 6:2 FTAB is known to induce  
358 developmental toxicity in zebrafish embryos (Shi et al., 2018) and 6:2 FTAB and 6:2 FtTAoS  
359 are known as a PFCAs precursors (D'Agostino and Mabury, 2014; Pan et al., 2018) which  
360 requires additional research on source and environmental fate. Due to a lower peak intensity,  
361 MS/MS spectra could not be acquired resulting in a CL 4 annotation confidence for those  
362 compounds. Also, it should be noted that the investigation of presence of isomer for CL 4  
363 compounds was limited due to the absence of MS/MS fragments.

364

### 365 3.3. Non-target Screening of PFAS

366 In influent wastewater samples from Belgium, seven PFAS homologue groups were  
367 identified which contained 2–3 compounds within a consecutive RT series (**Figure 2c**). Among  
368 these groups, 22 compounds from four homologue groups were identified with CL 1–3,  
369 whereas others remained at CL 5, because MS/MS spectra were not obtained (**Table S15**).

370 *Group 1–3.* Seven compounds were identified as PFSA group (group 1, **Figure S7a**)  
371 which comprises of trifluoromethanesulfonic acid (TFMS), perfluoropropanesulfonic acid  
372 (PFPrS), PFBS, perfluoropentanesulfonic acid (PFPeS), PFHxS, PFHpS, and PFOS (mass  
373 error: -0.5 to 6 ppm). The MS/MS fragmentation pattern of PFBS confirmed that these  
374 compounds are classified within the PFSA group. Shorter chain PFSA, such as TFMS, PFPrS,  
375 PFPeS, and PFHpS were found by homologue analysis without reference standards. Seven  
376 compounds were confirmed as PFCA group (group 2, **Figure S7b**) including



377 perfluoropropanoic acid (PFPrA), PFBA, PFPeA, PFHxA, PFHpA, PFOA, and PFNA (mass  
378 error: -0.5 to -9.3 ppm). The MS/MS fragmentation pattern of PFOA confirmed that these  
379 compounds are included in PFCA group. PFPrA was newly identified by homologue analysis.  
380 Group 3 included four compounds of the fluorotelomer sulfonates (FTS) group (**Figure S7c**),  
381 which consisted of 4:2, 6:2, 8:2, and 10:2 FTS and the MS/MS fragmentation pattern was  
382 confirmed with 6:2 FTS. Considering the PFSA, PFCA, and FTS groups as commonly  
383 monitored PFAS in the environmental matrices, our results showed that the non-target  
384 screening broadens the compound monitoring scope.

385 *Group 4.* Four compounds were identified as group 4 (potential name: n:3  
386 fluorotelomer unsaturated carboxylic acid (n:3 FTUCA or n:3 Uacids); C4–C7; mass error: -6.2  
387 to 1.2 ppm) characterized by the successive losses of CO<sub>2</sub> and C<sub>2</sub>H<sub>2</sub> and the presence of fully  
388 fluorinated carbon chain [C<sub>n</sub>F<sub>2n+1</sub>]<sup>-</sup> ions (**Figure S7d**). The MS/MS fragmentation patterns were  
389 obtained from C<sub>8</sub>H<sub>3</sub>F<sub>11</sub>O<sub>2</sub> (*m/z* 338.9852, -4.35 ppm) and C<sub>10</sub>H<sub>3</sub>F<sub>15</sub>O<sub>2</sub> (*m/z* 438.9813, -0.63 ppm)  
390 which confirmed their inclusion in the same homologue group. In previous studies, n:3 FTUCA  
391 has reported as an intermediate environmental transformation product (e.g., microbial  
392 biodegradation, biotransformation, etc.) of FTOHs such as 6:2 FTOH and 8:2 FTOH which are  
393 the principal materials for manufacturing FTOH-based products (Prevedouros et al., 2006;  
394 Zhang et al., 2013). In the earlier stage of degradation/transformation pathway of 6:2 FTOH  
395 and 8:2 FTOH, 5:3 FTUCA and 7:3 FTUCA are generated and PFCAs such as PFBA, PFPeA,  
396 PFHxA, PFHpA, and PFOA are known to be formed as final products. (Wang et al., 2005;  
397 Zhang et al., 2013; Zhao et al., 2013) In WWTP Deurne, the peak abundances of formulae  
398 C<sub>8</sub>H<sub>3</sub>F<sub>11</sub>O<sub>2</sub> (5:3 FTUCA) and C<sub>10</sub>H<sub>3</sub>F<sub>15</sub>O<sub>2</sub> (7:3 FTUCA) were approximately 10 times higher than  
399 other homologues which may be associated a higher concentration of PFCAs in WWTP  
400 Deurne. This result implies that there might be an input of FTOH or FT-based chemicals to  
401 WWTP Deurne, even though other degradation/transformation products were not observed.

402 *In-source fragmentation.* Recently, Kang et al. (2021) raised a concern that ions  
403 generated from the in-source fragmentation of PFCAs might have been classified as a new  
404 homologue group, such as unsaturated perfluoroalcohol (UPFA) (Kang et al., 2021; Wang et

405 al., 2018; Yu et al., 2021). The UPFA homologue group was also found in influent wastewater  
406 of Belgium, however, we found the possibility that these compound groups are closely  
407 associated with in-source fragmentation which could be induced during electrospray ionization.  
408 This phenomenon was observed through the comparison of injection results between native  
409 standard and wastewater sample from Deurne which showed the highest concentration of  
410 PFCAs (**Figure S8–S9**). As presented in **Figure S8–S9**, the peaks of PFCA ( $C_nHF_{2n-1}O_2$ ) and  
411 UPFA (loss of  $CF_2O$  from PFCA) were present at the same retention time as from native  
412 standard injection and WWTP Deurne. These data imply that the findings of UPFA from  
413 previous studies might have resulted from in-source degradation of PFCAs. Although Yu et al.  
414 (2021) suggested that UPFA might be generated as PFAS degradation intermediate with  
415 electrochemical oxidation or ultraviolet-generated hydrated electrons (Yu et al., 2021), careful  
416 investigation of PFCA-related homologue group will be needed in further studies.

417

#### 418 *3.4. Spatial trends of emerging PFAS*

419 The semi-quantified result for newly found PFAS is presented in **Table S16**.  
420 The mass load and relative contribution of 4 individual PFAS (annotated as CL 2a and 2b) and  
421 1 PFAS group (n:3 FTUCA) identified by suspect and non-target screening from Belgian  
422 WWTPs are shown in **Figure 2d** and **2e**. Similar to legacy PFAS, WWTP Deurne (117 g/day)  
423 showed the highest mass load of emerging PFAS followed by WWTPs of Leuven (9.69 g/day),  
424 Ghent (3.45 g/day), and Bruges (2.69 g/day). In all sites, 1:2 H-PFESA and AFFF-derived  
425 PFAS such as 6:2 FtSOAoS and 6:2 FtSO<sub>2</sub>AoS were detected indicating wide distribution of  
426 those compounds in influent wastewaters of Belgium. Overall, the dominant emerging PFAS  
427 in Belgian wastewater was 1:2 H-PFESA which represented 41% (WWTP Boom) to 99%  
428 (WWTP Mechelen) of total emerging PFAS, except for WWTP Deurne (0.8%). The distribution  
429 of other emerging PFAS was varied among sites, for instance, a higher contribution (38%) of  
430 bis(1,1,2,2,3,3,4,4,4-nonafluoro-1-butanefluoronyl)-imide was observed in WWTP Leuven,  
431 whereas n:3 FTUCA (group 4) were found as being the dominant emerging PFAS (99%) in  
432 WWTP Deurne. In WWTPs of Boom, Bruges, and Genk, 6:2 FtSOAoS and 6:2 FtSO<sub>2</sub>AoS were

433 higher than other PFAS which made up 48–60% of total emerging PFAS and which requires  
434 further in-depth investigation on contamination source (e.g., AFFF-impacted water) in those  
435 regions. Similar PFAS trends were found among time-trend samples in WWTP Brussels which  
436 were dominated by 1:2 H-PFESA indicating there might be less specific additional PFAS  
437 sources during the sampling periods.

438

### 439 3.5. Estimated population exposure

440 To estimate population exposure to investigated PFAS in study areas of Belgium,  
441 population-normalized mass load (PNML;  $\mu\text{g}\cdot\text{day}^{-1}\text{ person}^{-1}$ ) of legacy (sum of PFBS, PFHxS,  
442 PFOS, PFBA, PFPeA, PFHxA, PFHpA, PFOA, PFNA, PFDA, 8:2 FTS, and 10:2 FTS) and  
443 emerging PFAS (sum of 1:2 H-PFESA, 6:2 FtSOAoS, 6:2 FtSO<sub>2</sub>AoS, bis(1,1,2,2,3,3,4,4,4-  
444 nonafluoro-1-butanesulfonyl)-imide, C<sub>7</sub>H<sub>3</sub>F<sub>9</sub>O<sub>2</sub>, C<sub>8</sub>H<sub>3</sub>F<sub>11</sub>O<sub>2</sub>, C<sub>9</sub>H<sub>3</sub>F<sub>13</sub>O<sub>2</sub>, and C<sub>10</sub>H<sub>3</sub>F<sub>15</sub>O<sub>2</sub>;  
445 compounds annotated as CL 2a and 2b in suspect screening and n:3 FTUCA) were calculated  
446 among 16 WWTPs (**Figure 3, Table S17**). Overall, the PNML of legacy PFAS (8.7–626  $\mu\text{g}\cdot\text{day}^{-1}$   
447  $\text{ person}^{-1}$ ) were in a higher range than that of emerging PFAS (0.7–550  $\mu\text{g}\cdot\text{day}^{-1}$   $\text{ person}^{-1}$ )  
448 considering all sites, implying that people in the studied areas are more exposed to legacy  
449 PFAS than emerging PFAS. The highest PNML of legacy and emerging PFAS was found in  
450 WWTP Deurne (626  $\mu\text{g}\cdot\text{day}^{-1}$   $\text{ person}^{-1}$  for legacy PFAS and 550  $\mu\text{g}\cdot\text{day}^{-1}$   $\text{ person}^{-1}$  for emerging  
451 PFAS) which implied that populations in the catchment region of Deurne might be exposed to  
452 elevated PFAS levels compared to other regions.

453 Estimation of human exposure to PFAS using PNML has limitations because there is  
454 a lack of clear metabolic biomarker for PFAS, which means that human and other  
455 environmental sources (i.e., industrial) are indistinguishable (Choi et al., 2018). Therefore, the  
456 PNML values calculated from wastewater might not reflect the population exposure alone, but  
457 also the input from other sources. In addition to this, the semi-quantification approach used to  
458 calculate concentrations of emerging PFAS could result in under- or overestimation of  
459 exposure risks derived from the uncertainties of this method (i.e., differing response factors  
460 between compounds and/or instruments). Nevertheless, the monitoring of PFAS using

461 wastewater gives an opportunity to identify regions with relatively higher exposure risks and  
462 specific source input to develop further monitoring and management schematics.

463

#### 464 **4. Conclusions**

465 In our study, various legacy and emerging PFAS groups were monitored in municipal  
466 influent wastewater from Belgium located in the most populated areas and as a result,  
467 information on levels, patterns, spatio-temporal distribution, and population-normalized mass  
468 loads in each WWTP were provided. The major findings of our study are (1) the dominance of  
469 PFBA and PFPeA in the majority of Belgian wastewaters, (2) higher contribution of PFOA in  
470 WWTP Deurne (potential specific source indication), (3) occurrence of AFFF-derived PFAS in  
471 all Belgian WWTPs, and (4) the detection of n:3 FTUCA group (degradation/transformation  
472 product of FTOHs) in WWTP Deurne. The observation of n:3 FTUCA may imply the input of  
473 FTOHs in WWTP Deurne. Throughout the study, we confirmed that wastewater is a good  
474 indicator in investigating the contamination patterns and application of suspect and non-target  
475 screening to wastewater gives an opportunity to early-warning of emerging PFAS exposure to  
476 specific regions where people might have higher risks. The developed workflow can be applied  
477 to identify other groups of PFAS (i.e., zwitterionic) to extend the monitoring scope. Suspect  
478 and non-target screening in wastewaters can be effectively used to determine the site which  
479 needs further *in-depth* investigation as well as establishment of future regulations and/or  
480 management strategies on chemicals of emerging concern.

481

#### 482 **Acknowledgements**

483 The authors would like to thank the WWTP personnel from Aquafin (Belgium) and Aquarius  
484 (Belgium) for providing wastewater samples and Prof. Hyo-Bang Moon for sharing some of the  
485 PFAS native standards used for this study. Yunsun Jeong is funded by European Union's  
486 Horizon 2020 FET-OPEN programme, project number 829047, triboREMEDY. Katyeny  
487 Manuela Da Silva acknowledges a doctoral fellowship BOF DOCPRO 4 from the University of  
488 Antwerp. Elias Iturraspe is funded by the Research Scientific Foundation Flanders (FWO) -

489 project number 1161620N. Yukiko Fujii acknowledges Grants-in-Aid for Scientific Research  
490 from the Japan Society for the Promotion of Science (16K00565 and 21K12262). Tim  
491 Boogaerts is funded by the European Union's Justice Programme - Drugs Policy Initiatives,  
492 EuSeME (project number: 861602). Jeremy Koelmel would like to acknowledge Agilent  
493 Technologies for their generous support and guidance, including an ACT-UR grant (Agilent  
494 Research Gift #4488) for PFAS software development and application.

495

#### 496 **CRedit authorship contribution statement**

497 **Yunsun Jeong**: Conceptualization, Methodology, Validation, Formal analysis, Investigation,  
498 Data Curation, Writing–Original Draft. **Katyeny Manuela Da Silva**: Methodology, Software,  
499 Data Curation, Writing–Review & editing. **Elias Iturraspe**: Methodology, Data Curation,  
500 Writing–Review & editing. **Yukiko Fujii**: Methodology, Validation, Investigation, Writing–  
501 Review & editing. **Tim Boogaerts**: Conceptualization, Investigation, Writing–Review & editing.  
502 **Alexander L.N. van Nuijs**: Conceptualization, Investigation, Writing–Review & editing,  
503 Supervision. **Jeremy Koelmel**: Methodology, Software, Writing–Review & editing. **Adrian**  
504 **Covaci**: Conceptualization, Methodology, Validation, Investigation, Writing–Review & editing,  
505 Supervision.

506 **References**

- 507 Aimuzi, R., Luo, K., Chen, Q., Wang, H., Feng, L., Ouyang, F., Zhang, J., 2019. Perfluoroalkyl  
508 and polyfluoroalkyl substances and fetal thyroid hormone levels in umbilical cord blood  
509 among newborns by prelabor caesarean delivery. *Environ. Int.* 130, 104929.  
510 <https://doi.org/10.1016/j.envint.2019.104929>
- 511 Baccarelli, A., Pfeiffer, R., Consonni, D., Pesatori, A.C., Bonzini, M., Patterson Jr, D.G.,  
512 Bertazzi, P.A., Landi, M.T., 2005. Handling of dioxin measurement data in the presence  
513 of non-detectable values: overview of available methods and their application in the  
514 Seveso chloracne study. *Chemosphere* 60, 898–906.  
515 <https://doi.org/10.1016/j.chemosphere.2005.01.055>
- 516 Barzen-Hanson, K.A., Roberts, S.C., Choyke, S., Oetjen, K., Mcalees, A., Riddell, N.,  
517 Mccrindle, R., Ferguson, P. L., Higgins, C.P., Field, J.A., 2017. Discovery of 40 classes  
518 of per-and polyfluoroalkyl substances in historical aqueous film-forming foams (AFFFs)  
519 and AFFF-impacted groundwater. *Environ. Sci. Tech.* 51, 2047–2057.  
520 <https://doi.org/10.1021/acs.est.6b05843>
- 521 Buck, R.C., Franklin, J., Berger, U., Conder, J.M., Cousins, I.T., De Voogt, P., Jensen, A.A.,  
522 Kannan, K., Mabury, S.A., van Leeuwen, S.P.J., 2011. Perfluoroalkyl and polyfluoroalkyl  
523 substances in the environment: terminology, classification, and origins. *Integr. Environ.*  
524 *Assess. Manag.* 7, 513–541. <https://doi.org/10.1002/ieam.258>
- 525 Chang, E.T., Adami, H.-O., Boffetta, P., Wedner, H.J., Mandel, J.S., 2016. A critical review of  
526 perfluorooctanoate and perfluorooctanesulfonate exposure and immunological health  
527 conditions in humans. *Crit. Rev. Toxicol.* 46, 279–331.  
528 <https://doi.org/10.3109/10408444.2015.1122573>
- 529 Chen, H., Munoz, G., Duy, S.V., Zhang, L., Yao, Y., Zhao, Z., Yi, L., Liu, M., Sun, H., Liu, J.,  
530 Sauv e, S., 2020. Occurrence and distribution of per-and polyfluoroalkyl substances in  
531 Tianjin, China: The contribution of emerging and unknown analogues. *Environ. Sci.*  
532 *Technol* 54, 14254–14264. <https://doi.org/10.1021/acs.est.0c00934>
- 533 Choi, P.M., Tscharke, B.J., Donner, E., O'Brien, J.W., Grant, S.C., Kaserzon, S.L., Mackie, R.,

534 O'Malley, E., Crosbie, N.D., Thomas, K. V, 2018. Wastewater-based epidemiology  
535 biomarkers: past, present and future. *TrAC Trends Anal. Chem.* 105, 453–469.  
536 <https://doi.org/10.1016/j.trac.2018.06.004>

537 Cousins, I.T., DeWitt, J.C., Glüge, J., Goldenman, G., Herzke, D., Lohmann, R., Miller, M., Ng,  
538 C.A., Scheringer, M., Vierke, L., Wang, Z., 2020. Strategies for grouping per- and  
539 polyfluoroalkyl substances (PFAS) to protect human and environmental health. *Environ.*  
540 *Sci. Process. Impacts* 22, 1444–1460. <https://doi.org/10.1039/D0EM00147C>

541 D'Agostino, L.A., Mabury, S.A., 2017. Certain perfluoroalkyl and polyfluoroalkyl substances  
542 associated with aqueous film forming foam are widespread in Canadian surface waters.  
543 *Environ. Sci. Technol.* 51, 13603–13613. <https://doi.org/10.1021/acs.est.7b03994>

544 D'Agostino, L.A., Mabury, S.A., 2014. Identification of novel fluorinated surfactants in aqueous  
545 film forming foams and commercial surfactant concentrates. *Environ. Sci. Technol.* 48,  
546 121–129. <https://doi.org/10.1021/es403729e>

547 Evich, M.G., Davis, M.J.B., McCord, J.P., Acrey, B., Awkerman, J.A., Knappe, D.R.U.,  
548 Lindstrom, A.B., Speth, T.F., Tebes-Stevens, C., Strynar, M.J., Wang, Z., Weber, E.J.,  
549 Henderson, W.M., Washington, J.W., 2022. Per- and polyfluoroalkyl substances in the  
550 environment. *Science.* 375, eabg9065. <https://doi.org/10.1126/science.abg9065>

551 Gaballah, S., Swank, A., Sobus, J.R., Howey, X.M., Schmid, J., Catron, T., McCord, J., Hines,  
552 E., Strynar, M., Tal, T., 2020. Evaluation of developmental toxicity, developmental  
553 neurotoxicity, and tissue dose in zebrafish exposed to GenX and other PFAS. *Environ.*  
554 *Health Perspect.* 128, 47005. <https://doi.org/10.1289/EHP5843>

555 Gallen, C., Bignert, A., Taucare, G., O'Brien, J., Braeunig, J., Reeks, T., Thompson, J., Mueller,  
556 J.F., 2022. Temporal trends of perfluoroalkyl substances in an Australian wastewater  
557 treatment plant: A ten-year retrospective investigation. *Sci. Total Environ.* 804, 150211.  
558 <https://doi.org/10.1016/j.scitotenv.2021.150211>

559 Gebbink, W.A., Van Asseldonk, L., Van Leeuwen, S.P.J., 2017. Presence of emerging per-and  
560 polyfluoroalkyl Substances (PFASs) in river and drinking water near a fluorochemical  
561 production plant in the Netherlands. *Environ. Sci. Technol.* 51, 11057– 11065.

562 <https://doi.org/10.1021/acs.est.7b02488>

563 Giesy, J.P., Kannan, K., 2002. Peer reviewed: perfluorochemical surfactants in the environment.  
564 Environ. Sci. Technol. 36, 146A-152A. <https://doi.org/10.1021/es022253t>

565 Gordon, S.C., 2011. Toxicological evaluation of ammonium 4, 8-dioxa-3H-perfluorononanoate,  
566 a new emulsifier to replace ammonium perfluorooctanoate in fluoropolymer  
567 manufacturing. Regul. Toxicol. Pharmacol. 59, 64–80.  
568 <https://doi.org/10.1016/j.yrtph.2010.09.008>

569 Houtz, E., Wang, M., Park, J.-S., 2018. Identification and fate of aqueous film forming foam  
570 derived per-and polyfluoroalkyl substances in a wastewater treatment plant. Environ. Sci.  
571 Technol. 52, 13212–13221. <https://doi.org/10.1021/acs.est.8b04028>

572 Jacob, P., A. Barzen-Hanson, K., Helbling, D.E., 2021a. Target and nontarget analysis of per-  
573 and polyfluoroalkyl substances in wastewater from electronics fabrication facilities. Environ.  
574 Sci. Technol. 55, 2346–2356. <https://doi.org/10.1021/acs.est.0c06690>

575 Jacob, P., Wang, R., Ching, C., Helbling, D.E., 2021b. Evaluation, optimization, and application  
576 of three independent suspect screening workflows for the characterization of PFASs in  
577 water. Environ. Sci. Process. Impacts 23, 1554–1565.  
578 <https://doi.org/10.1039/D1EM00286D>

579 Kang, Q., Li, Q., Wang, L., Jia, Y., Zhang, X., Hu, J., 2021. Comment on “Suspect and  
580 Nontarget Screening of Per-and Polyfluoroalkyl Substances in Wastewater from a  
581 Fluorochemical Manufacturing Park.” Environ. Sci. Technol. 55, 5589–5592.  
582 <https://doi.org/10.1021/acs.est.0c06917>

583 Koelmel, J.P., Paige, M.K., Aristizabal-Henao, J.J., Robey, N.M., Nason, S.L., Stelben, P.J., Li,  
584 Y., Kroeger, N.M., Napolitano, M.P., Savvaides, T., Vasiliou, V., Rostkowski, P., Garrett,  
585 T.J., Lin, E., Deigl, C., Jobst, K., Townsend, T.G., Godri Pollitt, K.J., Bowden, J.A., 2020.  
586 Toward comprehensive per- and polyfluoroalkyl substances annotation using  
587 FluoroMatch software and intelligent high-resolution tandem mass spectrometry  
588 acquisition. Anal. Chem. 92, 11186–11194.  
589 <https://doi.org/10.1021/acs.analchem.0c01591>



590 Kwiatkowski, C.F., Andrews, D.Q., Birnbaum, L.S., Bruton, T.A., DeWitt, J.C., Knappe, D.R.U.,  
591 Maffini, M. V, Miller, M.F., Pelch, K.E., Reade, A., Soehl, A., Trier, X., Venier, M., Wagner,  
592 C.C., Wang, Z., Blum, A., 2020. Scientific basis for managing PFAS as a chemical class.  
593 Environ. Sci. Technol. Lett. 7, 532–543. <https://doi.org/10.1021/acs.estlett.0c00255>

594 Lenka, S.P., Kah, M., Padhye, L.P., 2021. A review of the occurrence, transformation, and  
595 removal of poly- and perfluoroalkyl substances (PFAS) in wastewater treatment plants.  
596 Water Res. 199, 117187. <https://doi.org/10.1016/j.watres.2021.117187>

597 Lindstrom, A.B., Strynar, M.J., Libelo, E.L., 2011. Polyfluorinated compounds: past, present,  
598 and future. Environ. Sci. Technol. 45, 7954–7961. <https://doi.org/10.1021/es2011622>

599 Liu, Y., D'Agostino, L.A., Qu, G., Jiang, G., Martin, J.W., 2019. High-resolution mass  
600 spectrometry (HRMS) methods for nontarget discovery and characterization of poly- and  
601 per-fluoroalkyl substances (PFASs) in environmental and human samples. TrAC - Trends  
602 Anal. Chem. 121, 115420. <https://doi.org/10.1016/j.trac.2019.02.021>

603 Liu, Y., Dos, A., Pereira, S., Martin, J.W., 2015. Discovery of C5–C17 poly-and perfluoroalkyl  
604 substances in water by in-line SPE-HPLC-Orbitrap with in-source fragmentation flagging.  
605 Anal. Chem. 87, 4260–4268. <https://doi.org/10.1021/acs.analchem.5b00039>

606 Loos, M., Singer, H., 2017. Nontargeted homologue series extraction from hyphenated high  
607 resolution mass spectrometry data. J. Cheminform. 9, 12. <https://doi.org/10.1186/s13321-017-0197-z>

608

609 McDonough, C.A., Choyke, S., Ferguson, P.L., Dewitt, J.C., Higgins, C.P., 2020.  
610 Bioaccumulation of Novel Per- And Polyfluoroalkyl Substances in Mice Dosed with an  
611 Aqueous Film-Forming Foam. Environ. Sci. Technol. 54, 5700–5709.  
612 <https://doi.org/10.1021/acs.est.0c00234>

613 Munoz, G., Liu, J., Vo Duy, S., Sauv e, S., 2019. Analysis of F-53B, Gen-X, ADONA, and  
614 emerging fluoroalkylether substances in environmental and biomonitoring samples: A  
615 review. Trends Environ. Anal. Chem. 23, e00066.  
616 <https://doi.org/10.1016/j.teac.2019.e00066>

617 Munoz, G., Michaud, A.M., Liu, M., Vo Duy, S., Montenach, D., Resseguier, C., Watteau, F.,

618 Sappin-Didier, V., Feder, F., Morvan, T., Houot, S., Desrosiers, M., Liu, J., Sauvé, S. 2021.  
619 Target and nontarget screening of PFAS in biosolids, composts, and other organic waste  
620 products for land application in France. Environ. Sci. Technol.  
621 <https://doi.org/10.1021/acs.est.1c03697>

622 Nason, S.L., Koelmel, J., Zuverza-Mena, N., Stanley, C., Tamez, C., Bowden, J.A., Godri Pollitt,  
623 K.J., 2021. Software comparison for nontargeted analysis of PFAS in AFFF-contaminated  
624 soil. J. Am. Soc. Mass Spectrom. 32, 840–846. <https://doi.org/10.1021/jasms.0c00261>

625 Newton, S., McMahan, R., Stoeckel, J.A., Chislock, M., Lindstrom, A., Strynar, M., 2017. Novel  
626 polyfluorinated compounds identified using high resolution mass spectrometry  
627 downstream of manufacturing facilities near Decatur, Alabama. Environ. Sci. Technol. 51,  
628 1544–1552. <https://doi.org/10.1021/acs.est.6b05330>

629 Pan, Y., Zhang, H., Cui, Q., Sheng, N., Yeung, L.W.Y., Sun, Y., Guo, Y., Dai, J., 2018. Worldwide  
630 distribution of novel perfluoroether carboxylic and sulfonic acids in surface water. Environ.  
631 Sci. Tech. 52, 7621–7629. <https://doi.org/10.1021/acs.est.8b00829>

632 Phong Vo, H.N., Ngo, H.H., Guo, W., Hong Nguyen, T.M., Li, J., Liang, H., Deng, L., Chen, Z.,  
633 Hang Nguyen, T.A., 2020. Poly-and perfluoroalkyl substances in water and wastewater:  
634 A comprehensive review from sources to remediation. J. Water Process Eng. 36, 101393.  
635 <https://doi.org/10.1016/J.JWPE.2020.101393>

636 Prevedouros, K., Cousins, I.T., Buck, R.C., Korzeniowski, S.H., 2006. Sources, fate and  
637 transport of perfluorocarboxylates. Environ. Sci. Technol. 40, 32–44.  
638 <https://doi.org/10.1021/es0512475>

639 Ruan, T., Jiang, G., 2017. Analytical methodology for identification of novel per-and  
640 polyfluoroalkyl substances in the environment. TrAC Trends Anal. Chem. 95, 122–131.  
641 <https://doi.org/10.1016/j.trac.2017.07.024>

642 Schymanski, E., Jeon, J., Gulde, R., Fenner, K., Ruff, M., Singer, H.P., Hollender, J., 2014.  
643 Identifying Small Molecules via High Resolution Mass Spectrometry: Communicating  
644 Confidence. Environ. Sci. Technol. 48, 2097–2098. <https://doi.org/10.1021/es5002105>

645 Shi, G., Xie, Y., Guo, Y., Dai, J., 2018. 6: 2 fluorotelomer sulfonamide alkylbetaine (6: 2 FTAB),

646 a novel perfluorooctane sulfonate alternative, induced developmental toxicity in zebrafish  
647 embryos. *Aquat. Toxicol.* 195, 24–32. <https://doi.org/10.1016/j.aquatox.2017.12.002>

648 Tsugawa, H., Cajka, T., Kind, T., Ma, Y., Higgins, B., Ikeda, K., Kanazawa, M., VanderGheynst,  
649 J., Fiehn, O., Arita, M., 2015. MS-DIAL: data-independent MS/MS deconvolution for  
650 comprehensive metabolome analysis. *Nat. Methods* 12, 523–526.  
651 <https://doi.org/10.1038/nmeth.3393>

652 UNEP, 2019a. SC-9/12: Listing of perfluorooctanoic acid (PFOA), its salts and PFOA-related  
653 compounds.  
654 [http://chm.pops.int/Convention/ConferenceofthePartiesCOP/COPDecisions/tabid/208/D](http://chm.pops.int/Convention/ConferenceofthePartiesCOP/COPDecisions/tabid/208/Default.aspx)  
655 [efault.aspx](http://chm.pops.int/Convention/ConferenceofthePartiesCOP/COPDecisions/tabid/208/Default.aspx) (Accessed 15 January 2022)

656 UNEP, 2019b. POPRC-15/1: Perfluorohexane sulfonic acid (PFHxS), its salts and PFHxS-  
657 related compounds.  
658 [http://chm.pops.int/TheConvention/ThePOPs/ChemicalsProposedforListing/tabid/2510/](http://chm.pops.int/TheConvention/ThePOPs/ChemicalsProposedforListing/tabid/2510/Default.aspx)  
659 [Default.aspx](http://chm.pops.int/TheConvention/ThePOPs/ChemicalsProposedforListing/tabid/2510/Default.aspx) (Accessed 15 January 2022)

660 UNEP, 2009. SC-4/17: Listing of perfluorooctane sulfonic acid, its salts and perfluorooctane  
661 sulfonyl fluoride, Stockholm Convention on Persistent Organic Pollutants.  
662 [http://chm.pops.int/Convention/ConferenceofthePartiesCOP/COPDecisions/tabid/208/D](http://chm.pops.int/Convention/ConferenceofthePartiesCOP/COPDecisions/tabid/208/Default.aspx)  
663 [efault.aspx](http://chm.pops.int/Convention/ConferenceofthePartiesCOP/COPDecisions/tabid/208/Default.aspx) (Accessed 15 January 2022)

664 Wang, Q., Ruan, Y., Jin, L., Zhang, X., Li, J., He, Y., Wei, S., Lam, J.C.W., Lam, P.K.S., 2021.  
665 Target, nontarget, and suspect screening and temporal trends of per- and polyfluoroalkyl  
666 substances in marine mammals from the South China Sea. *Environ. Sci. Technol.* 55,  
667 1045–1056. <https://doi.org/10.1021/acs.est.0c06685>

668 Wang, S., Huang, J., Yang, Y., Hui, Y., Ge, Y., Larssen, T., Yu, G., Deng, S., Wang, B., Harman,  
669 C., 2013. First report of a Chinese PFOS alternative overlooked for 30 years: its toxicity,  
670 persistence, and presence in the environment. *Environ. Sci. Technol.* 47, 10163–10170.  
671 <https://doi.org/10.1021/es401525n>

672 Wang, X., Yu, N., Qian, Y., Shi, W., Zhang, X., Geng, J., Yu, H., Wei, S., 2020. Non-target and  
673 suspect screening of per- and polyfluoroalkyl substances in Chinese municipal

674 wastewater treatment plants. *Water Res.* 183, 115989.  
675 <https://doi.org/10.1016/j.watres.2020.115989>

676 Wang, Y., Yu, N., Zhu, X., Guo, H., Jiang, J., Wang, X., Shi, W., Wu, J., Yu, H., Wei, S., 2018.  
677 Suspect and nontarget screening of per-and polyfluoroalkyl substances in wastewater  
678 from a fluorochemical manufacturing park. *Environ. Sci. Technol.* 52, 11007–11016.  
679 <https://doi.org/10.1021/acs.est.8b03030>

680 Wang Z., DeWitt, J.C., Higgins, C.P., Cousins, I.T., 2017. A never-ending story of per- and  
681 polyfluoroalkyl substances (PFASs)? *Environ. Sci. Technol.* 51, 2508–2518.  
682 <https://doi.org/10.1021/acs.est.6b04806>

683 Wen, H.-J., Wang, S.-L., Chuang, Y.-C., Chen, P.-C., Guo, Y.L., 2019. Prenatal  
684 perfluorooctanoic acid exposure is associated with early onset atopic dermatitis in 5-year-  
685 old children. *Chemosphere* 231, 25–31.  
686 <https://doi.org/10.1016/j.chemosphere.2019.05.100>

687 Wikström, S., Lin, P.-I., Lindh, C.H., Shu, H., Bornehag, C.-G., 2020. Maternal serum levels of  
688 perfluoroalkyl substances in early pregnancy and offspring birth weight. *Pediatr. Res.* 87,  
689 1093–1099. <https://doi.org/10.1038/s41390-019-0720-1>

690 Yeung, L.W.Y., De Silva, A.O., Loi, E.I.H., Marvin, C.H., Taniyasu, S., Yamashita, N., Mabury,  
691 S.A., Muir, D.C.G., Lam, P.K.S., 2013. Perfluoroalkyl substances and extractable organic  
692 fluorine in surface sediments and cores from Lake Ontario. *Environ. Int.* 59, 389–397.  
693 <https://doi.org/10.1016/j.envint.2013.06.026>

694 Yu, N., Guo, H., Yang, J., Jin, L., Wang, X., Shi, W., Zhang, X., Yu, H., Wei, S., 2018. Non-  
695 target and suspect screening of per-and polyfluoroalkyl substances in airborne particulate  
696 matter in China. *Environ. Sci. Technol.* 52, 8205–8214.  
697 <https://doi.org/10.1021/acs.est.8b02492>

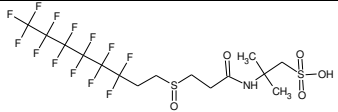
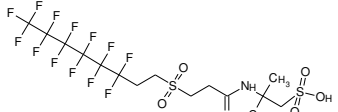
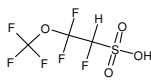
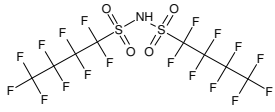
698 Yu, N., Wang, X., Li, Y., Jiao, Z., Wei, S., 2021. Response to Comment on “Suspect and  
699 Nontarget Screening of Per-and Polyfluoroalkyl Substances in Wastewater from a  
700 Fluorochemical Manufacturing Park.” *Environ. Sci. Technol.* 55, 5593–5596.  
701 <https://doi.org/10.1021/acs.est.1c01254>

702 Yukioka, S., Tanaka, S., Suzuki, Y., Echigo, S., Kärrman, A., Fujii, S., 2020. A profile analysis  
703 with suspect screening of per- and polyfluoroalkyl substances (PFASs) in firefighting foam  
704 impacted waters in Okinawa, Japan. *Water Res.* 184, 116207.  
705 <https://doi.org/10.1016/j.watres.2020.116207>

706 Zhang, S., Szostek, B., McCausland, P.K., Wolstenholme, B.W., Lu, X., Wang, N., Buck, R.C.,  
707 2013. 6:2 and 8:2 fluorotelomer alcohol anaerobic biotransformation in digester sludge  
708 from a WWTP under methanogenic conditions. *Environ. Sci. Technol.* 47, 4227–4235.  
709 <https://doi.org/10.1021/es4000824>

710 Zhao, L., McCausland, P.K., Folsom, P.W., Wolstenholme, B.W., Sun, H., Wang, N., Buck, R.C.,  
711 2013. 6:2 Fluorotelomer alcohol aerobic biotransformation in activated sludge from two  
712 domestic wastewater treatment plants. *Chemosphere* 92, 464–470.  
713 <https://doi.org/10.1016/j.chemosphere.2013.02.032>

714  
715**Table 1.** List of molecular formula, *m/z*, retention time (RT), identification score, diagnostic MS/MS fragments, confidence level, detection frequency (DF), and matched suspect list of compounds found in Belgian influent wastewaters.

No	Formula <sup>a</sup>	<i>m/z</i>	RT	Score <sup>b</sup> (highest)	MS/MS fragments (Diagnostic ion)	Confidence Level	DF (%)	List <sup>c</sup>	
1	C <sub>15</sub> H <sub>18</sub> F <sub>13</sub> NO <sub>5</sub> S <sub>2</sub>		602.0339	8.18	92 (99)	SI <sup>d</sup>	CL2a	100	*
2	C <sub>15</sub> H <sub>18</sub> F <sub>13</sub> NO <sub>6</sub> S <sub>2</sub>		618.0288	8.27	93 (99)	SI	CL2a	100	*
3	C <sub>3</sub> H <sub>2</sub> F <sub>6</sub> O <sub>4</sub> S		246.9498	4.68	85 (99)	SI (68.9, 146.9)	CL2b	100	***
4	C <sub>8</sub> HF <sub>18</sub> NO <sub>4</sub> S <sub>2</sub>		579.8974	8.30	95	SI	CL2b	5	*
5	C <sub>5</sub> H <sub>3</sub> Cl <sub>2</sub> F <sub>3</sub> O		204.9467	6.59	80 (93)	N.A. (Cl <sub>2</sub> confirmed)	CL3	100	*
6	C <sub>6</sub> H <sub>5</sub> Cl <sub>2</sub> F <sub>3</sub> O		218.9589	3.83	81 (93)	N.A. (Cl <sub>2</sub> confirmed)	CL3	62	*
7	C <sub>5</sub> H <sub>6</sub> BrF <sub>4</sub> NO <sub>2</sub>		265.9419	5.06	81 (92)	N.A. (Br confirmed)	CL3	76	*
8	C <sub>8</sub> H <sub>4</sub> BrF <sub>5</sub> O		288.9277	5.99	90	N.A. (Br confirmed)	CL3	5	*
9	C <sub>4</sub> H <sub>2</sub> F <sub>8</sub> O <sub>3</sub> S		280.9517	5.15	90	N.A. (79.96)	CL4	43	***
10	C <sub>7</sub> H <sub>6</sub> F <sub>9</sub> NO <sub>4</sub> S		369.9808	7.41	80 (95)	N.A.	CL4	81	**
11	C <sub>8</sub> HF <sub>15</sub> O <sub>3</sub> S		460.9323	8.16	78 (95)	N.A.	CL4	76	*, ***
12	C <sub>11</sub> H <sub>12</sub> F <sub>11</sub> NO <sub>4</sub> S		462.0265	6.01	80 (88)	N.A.	CL4	62	*
13	C <sub>15</sub> H <sub>19</sub> F <sub>13</sub> N <sub>2</sub> O <sub>4</sub> S		569.0777	8.66	95	N.A.	CL4	5	*
14	C <sub>15</sub> H <sub>18</sub> F <sub>13</sub> NO <sub>4</sub> S <sub>2</sub>		586.0378	8.43	90 (99)	N.A.	CL4	100	*

716  
717

<sup>a</sup>Formula used for find by formula option in Agilent MassHunter Qualitative Analysis 7.0; <sup>b</sup>Average Score obtained by Agilent MassHunter Qualitative Analysis 7.0; <sup>c</sup>Matched suspect list (\*PFAS Master List; \*\*PFASNTREV19; \*\*\*Previous studies); <sup>d</sup>Supporting Information.

**Figure 1.** Schematic diagram of data analysis workflow applied for suspect and non-target analysis of PFAS in Belgian wastewaters.

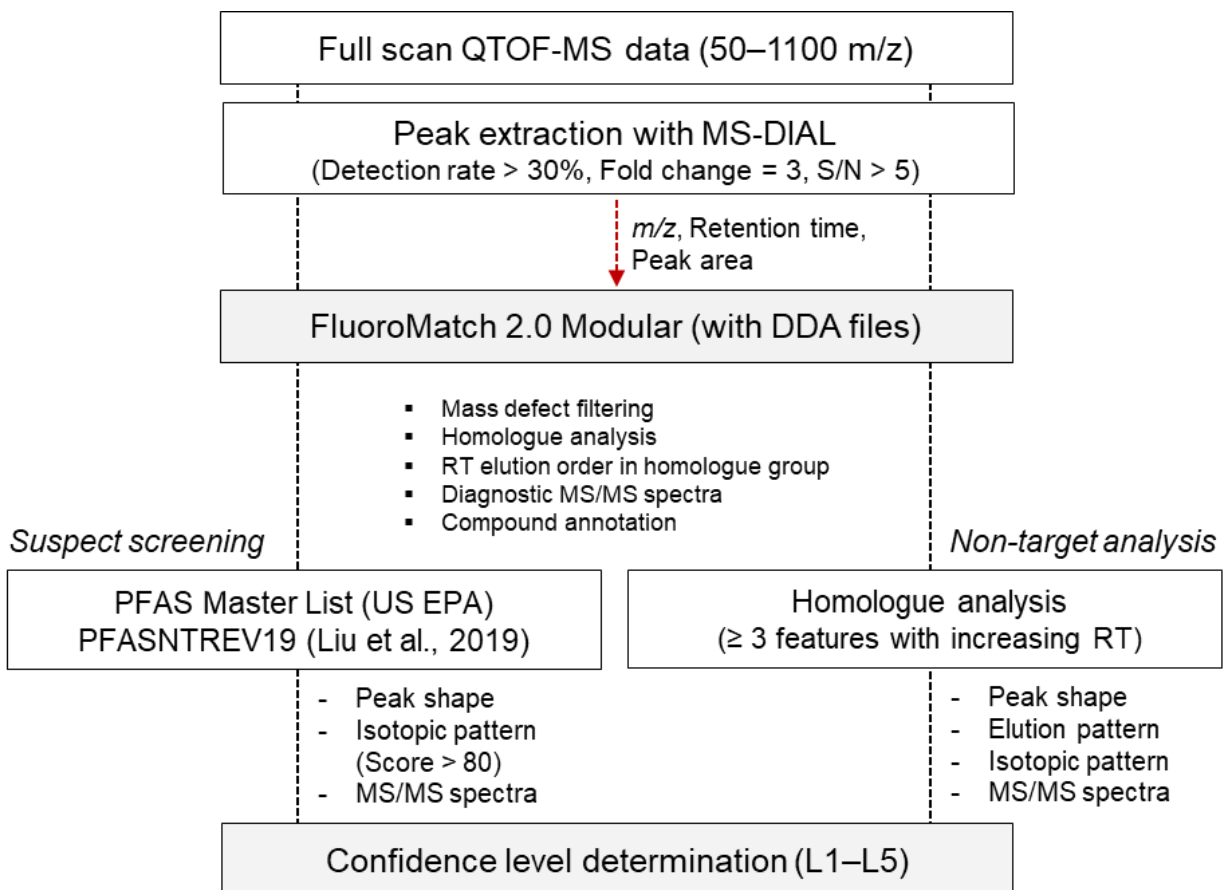


**Figure 2.** Concentration and contamination profiles of legacy and emerging PFAS in influent wastewater from 16 Belgian wastewater treatment plants (WWTPs) collected in 2020 and time-trend samples from WWTP Brussels (2013–2020). For the calculation of mass loads and contamination profiles of emerging PFAS, semi-quantification method was used. (a) mass load of legacy PFAS; (b) relative contribution of legacy PFAS; (c) PFAS homologue groups found by non-target screening; (d) mass load of emerging PFAS; (e) relative contribution of emerging PFAS.

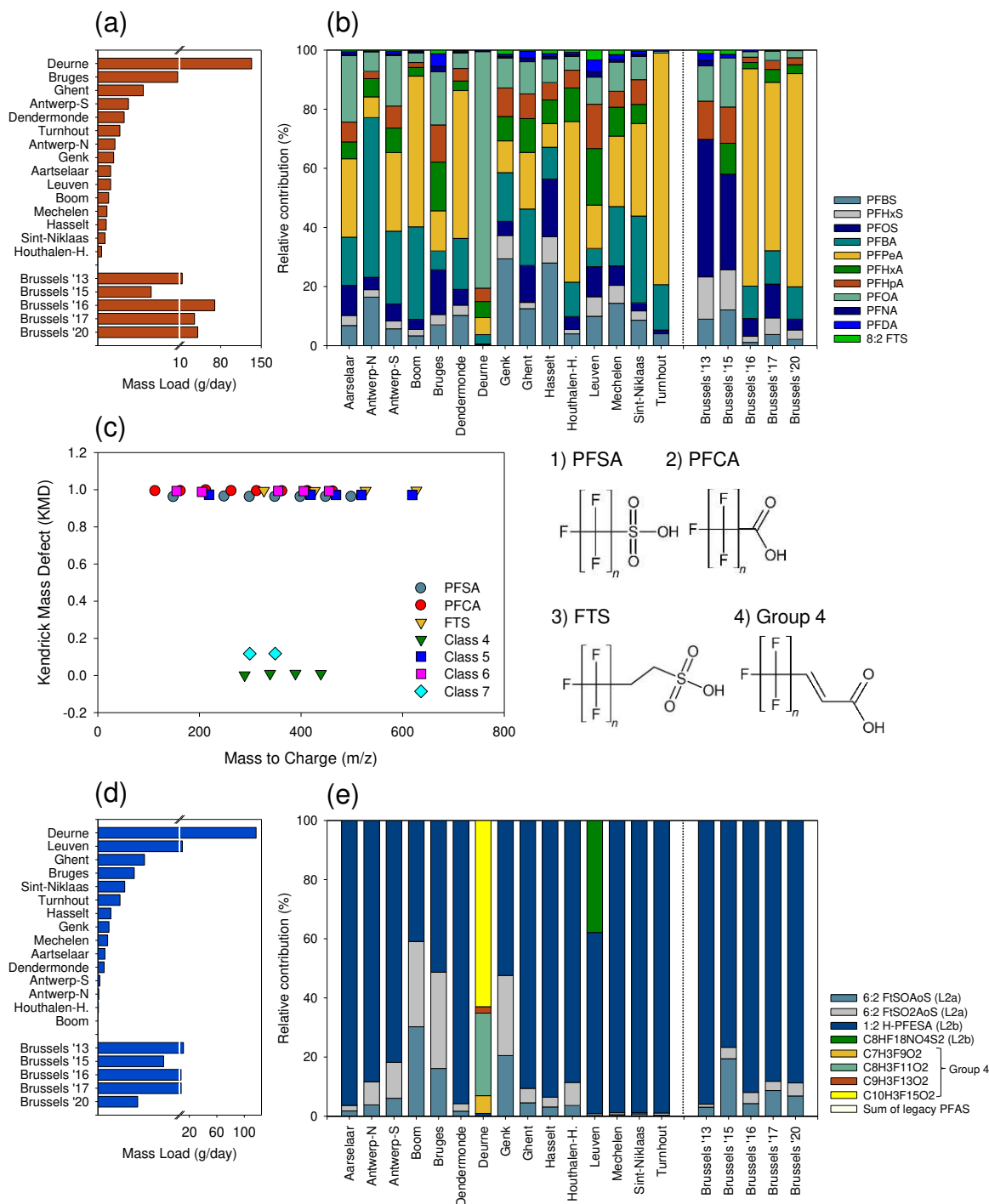




**Figure 3.** Calculated PNMLs (population normalized mass loads;  $\mu\text{g}\cdot\text{day}^{-1}\text{person}^{-1}$ ) in 16 Belgian WWTPs. Blue and yellow bars indicate the sum of PNML values for legacy (sum of 12 PFAS) and emerging PFAS (sum of 8 PFAS), respectively. Red dots and dashed lines indicate the location and name of WWTPs. Detailed values are presented in SI (Ant-N: Antwerp North, Ant-S: Antwerp South).

